Random magnetic anisotropy in thin films of amorphous $Mn_{48}B_{52}$

T. J. Kistenmacher, W. A. Bryden, and K. Moorjani
Milton S. Eisenhower Research Center, Applied Physics Laboratory, The Johns Hopkins University, Laurel, Maryland 20707-6099
(Received 24 February 1989)

While crystalline MnB is a ferromagnet ($T_c = 573$ K), rf diode-sputtered thin films of composition $Mn_{48}B_{52}$ are amorphous as ascertained by x-ray scattering and exhibit a low-field, hysteretic, static magnetization peak characteristic of a spin glass. High-field (up to 44 kG) static magnetization data at temperatures ranging between 6 and 200 K are analyzed within the random anisotropy model of Chudnovsky, Saslow, and Serota [Phys. Rev. B **33**, 251 (1986)]. In this model, the field-dependent magnetization at a given temperature is expressed as $M(H)=M(0)(1-CH^{-1/2})+\chi' H$, where the lead term follows from the analysis of a ferromagnet with a wandering axis (FWA) and the second term accounts for contributions from induced moments. The $T^{3/2}$ dependence of the saturation magnetization of the FWA contribution, $M(0)$, at low temperatures is suggestive of spin-wave excitations, while the temperature dependence of the fitting parameters C and χ' consistently identify several characteristic temperatures associated with the magnetic behavior of a-$Mn_{48}B_{52}$, including the low-field spin-glass transition temperature and Curie temperature and the curvature crossover temperature (established from a classical Arrott plot) that separates the FWA state and a pseudoparamagnetic limit.

I. INTRODUCTION

As part of our recent interest in the electrical transport and magnetic properties of amorphous Mn-B alloys,[1] extensive static susceptibility and magnetization data on a-$Mn_{48}B_{52}$ are reported here and interpreted within the random-anisotropy model of Chudnovsky, Saslow, and Serota (hereafter CSS).[2] In contrast to the ferromagnetism ($T_c = 573$ K) (Ref. 3) shown by crystalline MnB, a-$Mn_{48}B_{52}$ displays archetypal spin-glass behavior in the form of a low-field static susceptibility peak, with hysteresis. As the field strength increases, a new magnetic state evolves, and the field-dependent magnetization at a variety of temperatures ranging from 6 to 200 K has been qualitatively modeled by a summation of terms proportional to $H^{-1/2}$ and H. The former term arises from a ferromagnet with a wandering axis (FWA) (Ref. 2) and the latter from induced moments. A $T^{3/2}$ dependence for the derived saturation magnetization of the FWA contribution is suggestive of spin-wave excitations in the low-temperature regime.[4] Lastly, the derived fitting parameters within the CSS model consistently anticipate several characteristic magnetic temperatures, including the low-field spin-glass transition temperature and Curie temperature and the curvature crossover temperature discerned from a classical Arrott plot. Within the latter analysis, the crossover isotherm can be conveniently thought of as a pseudophase boundary separating near ferromagnetic (perturbed by the random anisotropy field) and near paramagnetic states.

II. EXPERIMENTAL RESULTS AND ANALYSIS

Thin films were prepared by rf diode sputtering of a 2:1 mole ratio of MnB and MnB_2 powders held in a tantalum cup. A secondary-ion mass spectroscopy analysis showed a resulting composition of $Mn_{48}B_{52}$ and less than 0.3% tantalum incorporation into the thin films. Substrates were high-purity fused quartz held at ~300 K during deposition. An x-ray scattering pattern (V filtered, Cr$K\alpha$ radiation), Fig. 1, showed two broad maxima centered at Q ($=4\pi \sin\theta/\lambda$) values of 3.16 and 5.10 Å^{-1} and was taken as an indication of an amorphous film deposition. The

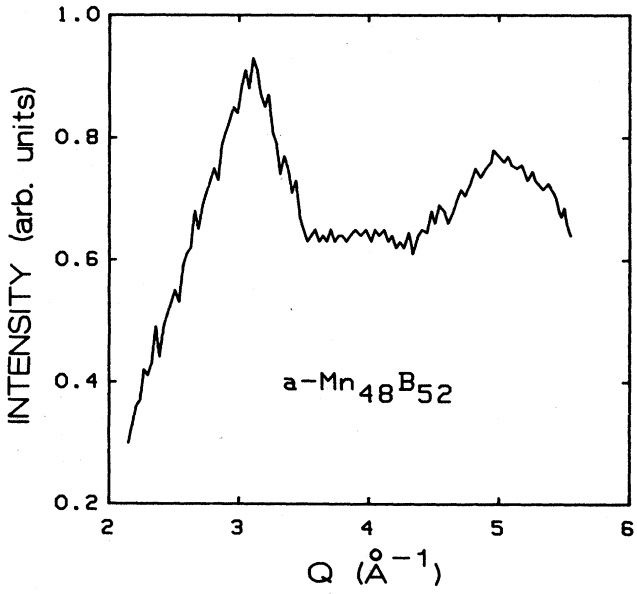

FIG. 1. X-ray scattering profile for a-$Mn_{48}B_{52}$.

sample selected for magnetic characterization was trapezoidal in shape (approximate area 4×10^{-2} cm^2) and 2 μm in thickness as determined from surface profilemetry.

Low-field magnetic susceptibility data were obtained by first cooling the sample to 6 K in zero field, and then warming to 72 K and subsequent cooling to 7 K in an applied field. All measurements were performed on a commercial SQUID magnetometer (S.H.E. Corporation) and analytically corrected for the miniscule contribution from the quartz substrate. Shown in Fig. 2(a) is the corrected static susceptibility at the lowest applied field of 5 G. On warming the zero-field cooled sample in the applied field, a distinct maximum in the static susceptibility is seen at 22.5 K. On cooling in the applied field, the data are strikingly congruent down to and slightly beyond the peak maximum, wherein hysteresis associated with spin-glass behavior intervenes. In Fig. 2(b), the inverse of the magnetic susceptibility at 5 G is plotted versus temperature. A linear least-squares fit well approximates the high-temperature data ($T>50$ K) and extrapolates to zero inverse susceptibility near 36 K.

Depicted in Fig. 3 are a set of static susceptibility measurements collected at increasing field strengths. Up to 315 G, there is sufficient resolution between the zero-field and field-cooled data to clearly recognize hysteretic effects. Empirically, there is a monotonic decrease in the peak position with increasing field, following a nominally linear dependence beyond 315 G [Fig. 4(a)]. Similarly, at lower applied fields, a logarithmic decrease in the magnitude of the susceptibility maximum [Fig. 4(b)] can be inferred, whereas saturation clearly sets in at the higher applied field strengths.

In Fig. 5, a series of isothermal (6–200 K) magnetization curves to a maximum field strength of 44 kG are presented. In general, this family of curves is seen to be reversible and approximately linearly dependent on the field strength at the highest applied fields. Of particular interest to these results is the theoretical analysis of Chudnovsky, Saslow, and Serota[2] for a ferromagnet with a wandering axis. The FWA model represents essentially an aligned state that is not quite ferromagnetic owing to the perturbation induced by random anisotropy. The field dependence at a given temperature of the magnetization of the FWA state is predicted[2] to have the following form:

$$M(H)=M(0)(1-CH^{-1/2}) , \tag{1}$$

with $M(0)$ the saturation magnetization of the FWA state and $C=\frac{1}{15}(H_r^4/H_{ex}^3)^{1/2}$, where H_{ex} is the exchange field and H_r is the random-anisotropy field. Addition of a

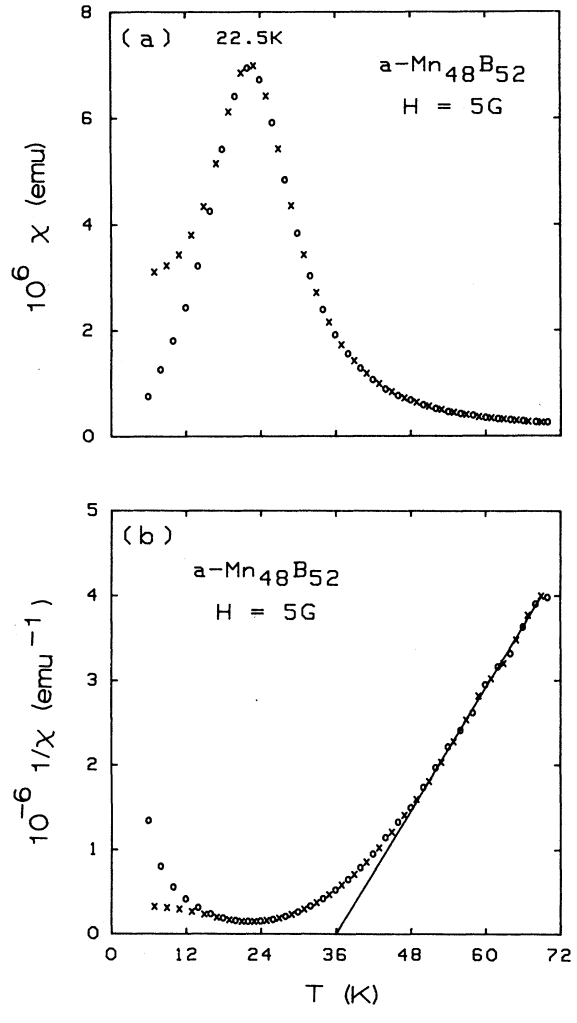

FIG. 2. (a) Temperature dependence of the low-field (5 G) magnetic susceptibility for a-$Mn_{48}B_{52}$ (○, increasing temperature; ×, decreasing temperature); (b) temperature dependence of the low-field (5 G) inverse magnetic susceptibility for a-$Mn_{48}B_{52}$. The superimposed line is a least-squares fit to the data above 50 K.

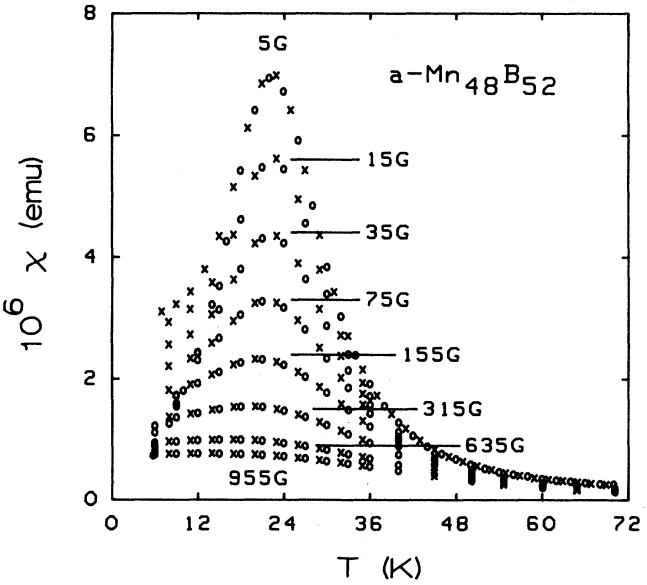

FIG. 3. Temperature dependence of the magnetic susceptibility for a-$Mn_{48}B_{52}$ at a variety of external field strengths.

term linear in H accounts for induced moments and leads to Eq. (2):

$$M(H)=M(0)(1-CH^{-1/2})+\chi' H \ . \quad (2)$$

A least-squares fit of Eq. (2) to the experimental data has been implemented, and the quality of the fit and the relative importance of each term are illustrated in Figs. 6(a)–6(c) for $T=6$, 60, and 200 K, respectively. While the magnetization at the lowest fields is always dominated by the FWA term, the contribution from induced moments clearly becomes the dominant factor (even at intermediate field strengths) at the higher temperatures. It is also to be noted that the somewhat poorer quality of the fit is not restricted to the 60 K data [Fig. 6(b)], but is congenital to the $T=60$–100 K regime.

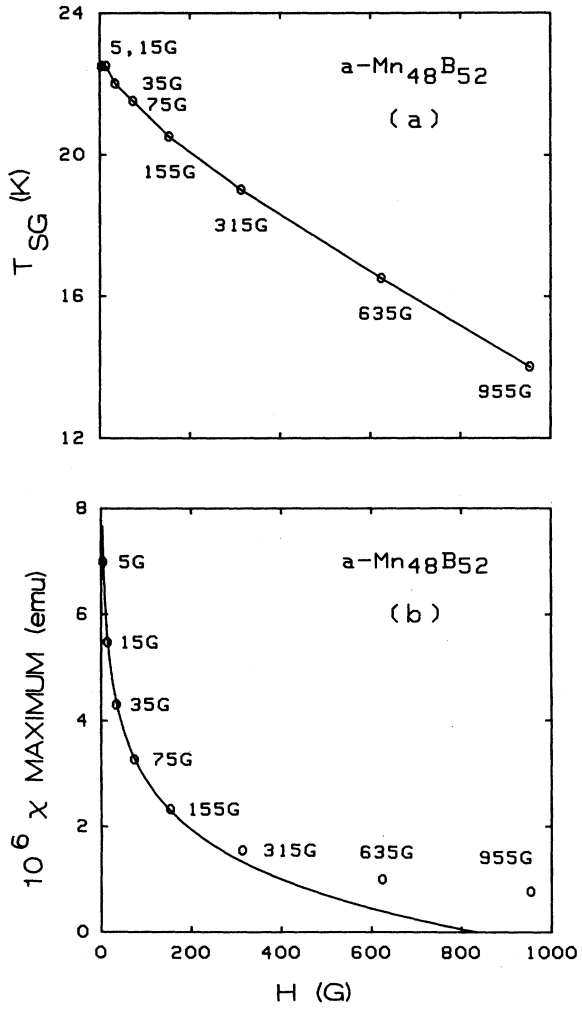

FIG. 4. (a) Dependence of the spin-glass transition temperature (T_{SG}) on field strength. The superimposed line is a guide to the eye; (b) dependence of the susceptibility maximum on field strength. The superimposed line is a logarithmic fit to the lower field data up to 155 G.

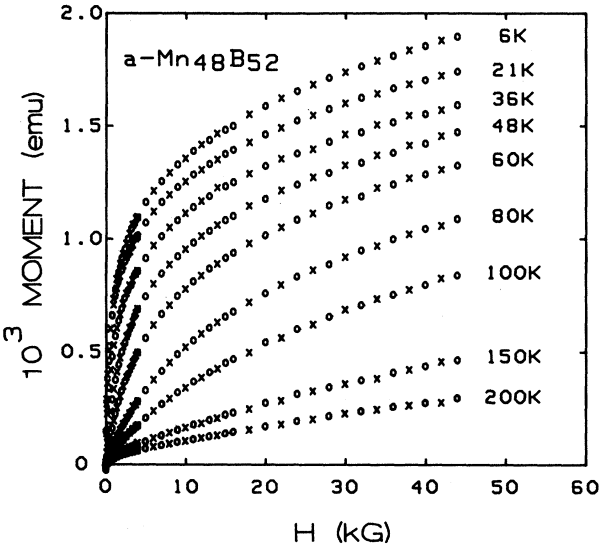

FIG. 5. Isothermal magnetization data (○, increasing field strength; ×, decreasing field strength) for a-$Mn_{48}B_{52}$ over a range of temperatures.

III. DISCUSSION

The similarities and contrasts between the magnetic properties of crystalline and amorphous manganese compounds are extensive and provocative. At the one extreme, c-MnAs ($T_c=318$ K) and c-MnSb ($T_c=587$ K) are strong ferromagnets and their amorphous films are either ferromagnetic or superparamagnetic depending on the preparative conditions.[5] At the other extreme, MnC does not exist as a stable crystalline compound and a-MnC is a concentrated magnetic glass with a spin-glass transition temperature T_{SG} of 21 K.

The most heavily studied of the binary manganese compounds has been MnSi, largely due to the unusual magnetic properties of its crystalline phase. Bulk c-MnSi displays a temperature-dependent susceptibility characteristic of a typical weak ferromagnet with a Curie temperature Θ of 36 K.[6] The field-dependent magnetization rises linearly up to 6.2 kG, where it saturates abruptly. Neutron diffraction and nuclear magnetic resonance data explicitly demonstrate that c-MnSi has a helical spin structure at zero field that evolves to a conical spin arrangement at higher field strengths.[6] The cone angle then decreases continuously with increasing field until the cone angle is zero at the saturation field of 6.2 kG. In sharp contrast, a-MnSi is a conventional magnetic spin glass with $T_{SG}=22$ K.[7]

Reflection on the crystalline and amorphous phase properties outlined above led Hauser[5] to suggest that weak ferromagnetism, ferrimagnetism, or antiferromagnetism in the crystalline phase is essential to the achievement of a spin-glass state in the amorphous phase. In contrast to this expectation, a-Mn-B alloys near a 1:1 composition have been recently shown to exhibit low-field spin-glass behavior[1] even though c-MnB is a strong ferromagnet ($T_c=573$ K).[3]

The low-field spin-glass state demonstrated here for amorphous films of $Mn_{48}B_{52}$ is distinguished by a spin-glass transition temperature (22.5 K) that is essentially identical to those shown by a-MnC (21 K) (Ref. 5) and a-MnSi (22 K).[7] Similarly, the low-field Curie temperature [$\Theta = 36$ K, Fig. 1(b)] for a-$Mn_{48}B_{52}$ is only slightly larger than that (30 K) exhibited by a-MnSi.[7] In fact, the similar values for T_{SG} and Θ for a-$Mn_{48}B_{52}$, a-MnC, and a-MnSi suggests origins in their common stoichiometry and probably analogous mean Mn-Mn interatomic distribution.

On increasing the applied magnetic field (Figs. 3 and

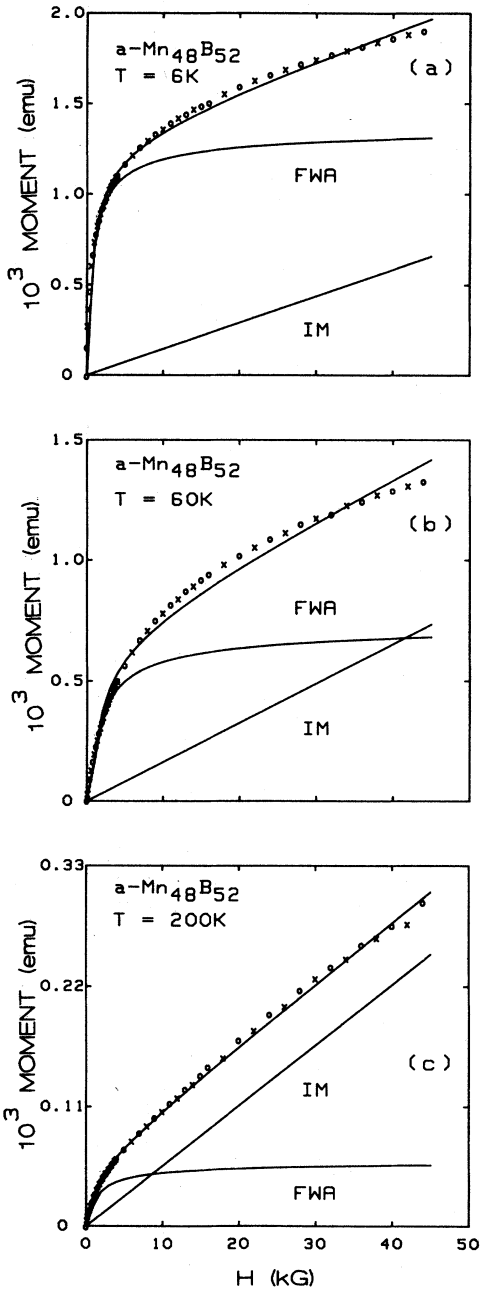

FIG. 6. Analytical fits of the CSS model to the isothermal magnetization data for a-$Mn_{48}B_{52}$ at (a) $T = 6$ K, (b) $T = 60$ K, and, (c) $T = 200$ K. Illustrated in each case are the relative contributions from a ferromagnet with a wandering axis and induced moments.

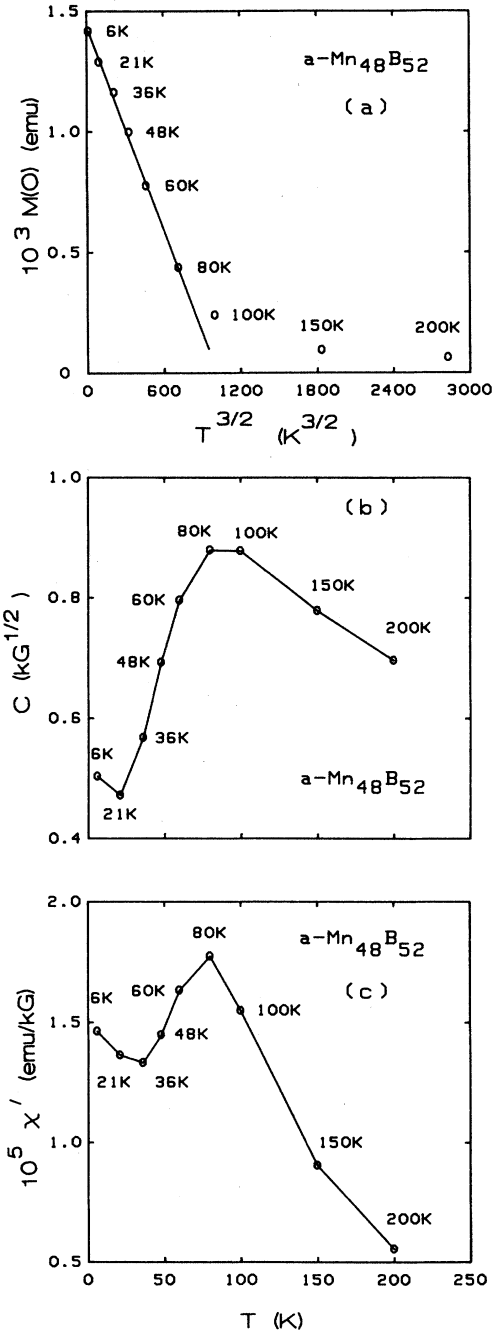

FIG. 7. Temperature dependence of the fitting parameters within the CSS model. (a) $M(0)$ with $T^{3/2}$. The superimposed line is a least-squares fit to the data up to 80 K. (b) C with T. The superimposed line is a guide to the eye. (c) χ' with T. The superimposed line is a guide to the eye.

4), the spin-glass transition temperature for a-$Mn_{48}B_{52}$ is suppressed to lower values and the susceptibility amplitude diminishes logarithmically, each of which is consistent with the evolution of an alternative magnetic state. One proposal for this new magnetic state is that of a ferromagnet with a wandering axis as described by Chudnovsky, Saslow, and Serota.[2] As outlined above, a least-squares fit of the experimental data to the isothermal FWA magnetization plus a term to account for induced moments [Eq. (2)] has been implemented at a variety of temperatures between 6 and 200 K. The temperature dependence of the fitting parameters within the CSS (Ref. 2) model are now briefly considered. In Fig. 7(a), the derived saturation magnetization, $M(0)$, for the FWA contribution to the magnetization is plotted as a function of $T^{3/2}$. As can be seen, $M(0)$ decreases linearly with $T^{3/2}$ at least up to 80 K and this dependence can be taken as an indication of some type of spin-wave excitations in the low-temperature regime.[1,4]

The variation of the coefficient C is nonmonotonic with temperature [Fig. 7(b)], with a local minimum indicative of the spin-glass transition temperature (22.5 K), and a local maximum suggestive of the temperature ($\sim$80 K) beyond which the dependence of $M(0)$ is no longer well represented by a $T^{3/2}$ law. Finally, in Fig. 7(c) the coefficient χ' of the induced moment term is shown to display a temperature dependence similar to that exhibited by C. Here, however, the local minimum occurs closer to the low-field Curie temperature (36 K) than the spin-glass transition temperature and the local maximum near 80 K is more sharply defined.

The consistent occurrence of a local maximum near 80 K for the temperature dependence of the fitting parameters C and χ' led us to consider other magnetic phenomena identified with this characteristic temperature. A classical Arrott plot of M^2 versus H/M showed the expected absence of mean-field behavior (H/M linear in M^2) and the curvature characteristic of random-anisotropy effects.[8] Explicitly, the isotherms at 48 and 60 K show moderate negative concavity, while the isotherm at 100 K exhibits a strong positive concavity. It was particularly noted that at moderate-to-large values of H/M the 80 K isotherm follows a near linear dependence implying that the curvature crossover temperature occurs near 80 K—the same characteristic temperature consistently identified in Fig. 7.

In the adapted FWA model employed here, the curvature crossover near 80 K cannot be equated with a critical line separating conventional ferromagnetic and paramagnetic phases. However, as the FWA state represents only a slight noncollinear perturbation on the normal ferromagnet, the 80-K isotherm can be conveniently thought of as a pseudophase boundary line separating near ferromagnetic and near paramagnetic states.

IV. SUMMARY

The magnetic properties of a-$Mn_{48}B_{52}$ have been extensively studied experimentally as a function of temperature and field strength. At low temperatures and low fields, the magnetic state is that of a concentrated spin glass. The magnetic parameters (T_{SG} and Θ) of the spin-glass state are similar to those associated with other amorphous manganese alloys derived from low atomic number metalloids (e.g., a-MnC and a-MnSi). At higher fields, a new magnetic state is attained and has been qualitatively analyzed within the FWA model of Chudnovsky, Saslow, and Serota.[2] The temperature dependence of the fitting parameters within this model identify several characteristic magnetic temperatures for both magnetic phases. Included amongst these are the low-field spin-glass temperature and Curie temperature and the pseudophase boundary between the FWA dominated state and a nearly paramagnetic state.

ACKNOWLEDGMENTS

Support of this research by the Department of the Navy under Contract No. N00039-87-C5301 is gratefully acknowledged. We thank Professor C. L. Chien for allowing us access to the SQUID magnetometer.

[1]W. A. Bryden, J. S. Morgan, T. J. Kistenmacher, and K. Moorjani, J. Appl. Phys. **61**, 3661 (1987); S. B. Liao, S. M. Bhagat, M. J. Park, M. A. Manheimer, K. Moorjani, and F. G. Satkiewicz, *ibid.* **61**, 3636 (1987).

[2]E. M. Chudnovsky, W. M. Saslow, and R. A. Serota, Phys. Rev. B **33**, 251 (1986). For earlier theoretical development, see E. M. Chudnovsky and R. A. Serota, J. Magn. Magn. Mater. **43**, 48 (1984); J. Phys. C **16**, 4181 (1983); Phys. Rev. B **26**, 2697 (1982).

[3]N. Lundquist and H. P. Meyers, Ark. Fys. **20**, 463 (1961); H. Hirota and A. Yanase, J. Phys. Soc. Jpn. **20**, 1596 (1965).

[4]K. Moorjani and J. M. D. Coey, *Magnetic Glasses* (Elsevier, Amsterdam, 1984).

[5]J. J. Hauser, Phys. Rev. B **22**, 2554 (1980).

[6]H. J. Williams, J. H. Wernick, R. C. Sherwood, and G. K. Wertheim, J. Appl. Phys. **37**, 1256 (1966); D. Shinoda and S. Asanabe, J. Phys. Soc. Jpn. **21**, 555 (1966); J. H. Wernick, G. K. Wertheim, and R. C. Sherwood, Mater. Res. Bull. **7**, 1431 (1972); Y. Ishikawa, K. Tajima, D. Bloch, and M. Roth, Solid State Commun. **19**, 525 (1976); K. Motoya, H. Yasuoka, Y. Nakamura, and J. H. Wernick, *ibid.* **19**, 529 (1976).

[7]J. J. Hauser, Solid State Commun. **30**, 201 (1979); R. W. Cochrane, J. O. Strom-Olsen, and J. P. Rebouillat, J. Appl. Phys. **50**, 7348 (1979); J. J. Hauser, F. S. L. Hsu, G. W. Kammlott, and J. V. Waszczak, Phys. Rev. B **20**, 3391 (1979).

[8]A. Aharony and E. Pytte, Phys. Rev. Lett. **45**, 1583 (1980).